Cascade decay of atomic magnesium after photoionization with a photoelectron-photoion coincidence method

B. Kanngießer, W. Malzer, M. Müller, N. Schmidt, and P. Zimmermann
Institut für Atomare Physik und Lehrerbildung, Technische Universität Berlin, Hardenberstraße 36, 10623 Berlin, Germany

A. G. Kochur and V. L. Sukhorukov
Rostov State University of Transport Communication, Rostov-na-Donu, 344038, Russia
(Received 2 May 2003; published 13 August 2003)

For the *K*-shell decay, magnesium is the first element in the periodic table which shows cascading transitions. We investigated the whole cascade of magnesium by using the photoelectron-photoion coincidence technique on the $1s$, $2s$, and $2p$ decay. The experimentally determined and calculated decay probabilities for the $1s^{-1}$, the $2s^{-1}$, and the $2p^{-1}$ decay, i.e., the whole cascade, are in good agreement with each other. For the calculation of higher final ionic charge states, it was found that electron correlations have to be taken into account. The fluorescence yields for the *K* and *L* shell and the Coster-Kronig factor for the *L* shell were determined.

DOI: 10.1103/PhysRevA.68.022704 PACS number(s): 32.80.Fb, 32.80.Hd

I. INTRODUCTION

For the last decade the photoelectron-photoion coincidence technique (PEPICO) with energy-analyzed electrons has been used successfully to investigate the complex decay routes after inner-shell photoionization. This technique not only delivers the quantitative determination of decay probabilities but also can disentangle in its extended form, various photoionization processes, leading to same final ionic charge state [1]. Especially for the investigation of the decay of shallow inner shells, the extended form of PEPICO, which we call final ion-charge resolving electron (FIRE) spectroscopy, proved to be a very versatile tool to separate discrete and continuous photoionization processes [2]. The decay of shallow inner shells is dominated by electronic decay to final ionic states with a charge higher than two, whereas the radiative decay is negligible for these decays.

Nevertheless, we also used the photoelectron-photoion coincidence technique for the determination of *K*-shell fluorescence yields of light elements [3,4]. As fluorescence yields are of growing interest for analytical methods, we proposed a way to determine fluorescence yields and Auger decay probabilities quantitatively with PEPICO [4] for all elements. If there are no cascade processes in the deexcitation, the ratio of radiative to nonradiative transitions or the ratio of single to double Auger transitions can be directly related to the corresponding ratios of the final ionic charge states. For cascading transitions, however, additional coincidence measurements are needed. With respect to the *K*-shell decay, magnesium ($1s^2 2s^2 2p^6 3s^2$) is the first element in the periodic table which shows these cascading transitions. Thus, we investigated the whole cascade of magnesium by using the PEPICO technique on the $1s$, $2s$, and $2p$ decay. The undulator beam line U41-PGM at BESSY delivered enough flux to realize these measurements on free magnesium atoms in the whole energy range needed, i.e., at 1400 eV for the $1s$ decay and at 170 eV for the $2s$ and $2p$ decay.

II. EXPERIMENT

A. The experimental setup

The investigation of the whole cascade decay of magnesium was carried out at the high flux undulator beamline U41 with a plane grating monochromator at the electron storage ring BESSY II in Berlin, Germany. An atomic beam was produced in an oven where the magnesium metal was heated to evaporation. The photoionization process investigated is determined by those photoelectrons with the respective kinetic energy. The electrons are measured with a cylindrical mirror analyzer under the magic angle. The photoelectrons with the corresponding kinetic energy serve as start signals for ion time-of-flight (TOF) measurements, in which the ions are separated according to their mass-to-charge ratio. The photoions measured are registered in the coincidence spectrum. Thus, final ionic charge states are correlated to a certain initial state. A full description of the experimental setup can be found in Ref. [5].

B. The coincidence measurements

The coincidence spectra measured do not contain directly the correlation probabilities $p\ (\epsilon, n+)$ of the final ionic charge states $n+$ to the initial state selected by the kinetic energy ϵ of the electrons. The spectra have to be corrected for false starts and false coincidences, the dead time in the coincidence signal registration, the finite transmission of the TOF spectrometer, and the detection efficiency of the ion detector. The transmission and the detection efficiency of the TOF spectrometer differ for the ionic charge states resulting in a relative discrimination of ions with lower charge state. Simulations of the ion trajectories inside the TOF showed that these effects can be neglected for light elements, for example, Ne, Na, and Mg. The correction for false coincidences is carried out by the measurement of reference TOF spectra under the same experimental conditions started with randomly generated pulses. Spectra of true coincidences are obtained by subtracting the reference spectra from the coin-

cidence spectra whereby dead time effects are taken into account. A detailed description of this statistical evaluation procedure can be found in Ref. [6]. But even after the correction procedures already described, the correlation probabilities $p(\epsilon,n+)$ obtained may deviate from the decay probabilities $P(nl^{-1}\rightarrow n+)$ of the corresponding core hole state nl^{-1}. This can be caused by a continuous energy distribution of electrons in the electron spectra produced in such processes as direct double photoionization or direct double Auger decay. The contribution of these processes to start pulses in the coincidence measurements can be extracted by our method of FIRE spectroscopy. Here, the respective coincidence spectra are taken not only at the maximum of the photoelectron peak but also at other electron energies in the peak and on the background. Thus, a complete photoelectron peak can be decomposed into parts that are correlated to certain final ionic charge states. The decomposition of the peak area is carried out by multiplying each correlation probability with the signal intensity of the electron energy on which the coincidence has been measured and using a normalization relation for the sum of the respective correlation probabilities. The decay probabilities are obtained from the areas of the decomposed photoelectron peak. Thus, the contribution from processes leading to a continuous energy distribution is separated from the photoionization process. An example of the FIRE method which describes the method in detail is given in Ref. [5].

C. Determination of fluorescence yields and Auger decay probabilities

In the photoionization process, a radiative decay can be distinguished from a nonradiative one by comparing the charge state of the initial state to that of the final state. If the photoion coincidence signal has the same charge state as the initial state designated from the photoelectron, only the emission of a fluorescence photon could have taken place. In contrast, each increase of the final charge state indicates the emission of Auger or Coster-Kronig electrons. We use the difference in the final charge state to determine fluorescence yields and Auger decay probabilities. A general outline of the method is given in Ref. [4]. For the case of noncascading transitions, one type of photoelectron-photoion coincidence measurement is sufficient to determine the fluorescence yield and the Auger and Coster-Kronig decay probabilities. We already succeeded to determine the decay probabilities of the *K* shell for Neon and Sodium [3,4].

Magnesium ($1s^2 2s^2 2p^6 3s^2$), the next element in the periodic table, is the first element which shows cascading transitions after $1s$ photoionization. Thus, additional coincidence measurements are necessary to determine decay probabilities. We investigated the whole cascade process of magnesium after $1s$ photoionization by carrying out photoelectron-photoion coincidence measurements on the $1s$, $2s$, and $2p$ decay. The results of these investigations are described in the Sec. IV.

III. THEORETICAL CALCULATIONS

The decays of $2p$, $2s$, and $1s$ vacancies in Mg are simulated in one-electron configuration-average approximation [7,8]. Many-electron correlations which may lead to double Auger processes (DAP) are not expected to be of great importance here. The reason for that is the small number of valence electrons, while simple statistical considerations show that the DAP probability depends on the number of valence electrons with N^3. Since in Ne, with eight outer-shell electrons, the DAP probability is about 6% [3], one can roughly estimate the amount of DAP in Mg to be about 0.6%. This is a small amount, however, one can try to detect it if double processes contribute only to a specific ionic state which cannot be reached otherwise. This happens upon the decay of the Mg $2s$ vacancy, where only $2+$ can be produced with diagram transitions. Therefore, in the description of the decay of the Mg $2s$ vacancy, we go beyond the one-electron configuration-average approximation and include electron correlation to account for the formation of triply charged photoions.

In the one-electron configuration-average approximation, only diagram radiative and nonradiative transitions are considered. For every branching point of a decay tree (i.e., initial or intermediate decaying configuration) the partial radiative and nonradiative decay widths are calculated as described in Ref. [8]. Transition energies entering the expressions for the transition widths are calculated as differences of total configuration-average Pauli-Fock energies of initial and final ionic states. If configuration C can decay into a number of final state configurations C_k, then each of these decays is characterized by the branching ratio

$$\chi(C\rightarrow C_k)=\frac{\Gamma(C\rightarrow C_k)}{\sum_k \Gamma(C\rightarrow C_k)}, \tag{1}$$

where $\Gamma(C\rightarrow C_k)$ are the partial decay widths. After a decay tree is constructed the probability of the formation of an ion of a specific charge $n+$ can be found as a sum of probabilities for all decay pathways leading from the initial configuration to the $n+$ state. For a specific pathway, the probability is a product of branching ratios of consecutive transitions. In the case of $2s$ vacancy decay, the following many-electron correlations have been considered (see Table II):

(1) correlations of the core electrons;

(2) correlations of the core with the Auger and Coster-Kronig electrons; i.e., inelastic scattering of Auger and Coster-Kronig electrons by core electrons.

Correlations of the core can be subdivided into two categories, i.e., monopole (or shake) excitations which are due to the change of the core potential. Then, one of the outer-shell core electrons is shaken up or off without any change of its orbital momentum. The other category contains nonmonopole correlations which have correlation states with two excited electrons. Monopole shake processes are included in the frame of the sudden perturbation approach (see Ref. [9] and references therein). Both, nonmonopole correlations of the core electrons and correlations of the core and the Auger electrons are accounted for within the first-order perturbation theory (PT) for the wave functions. In an earlier publication

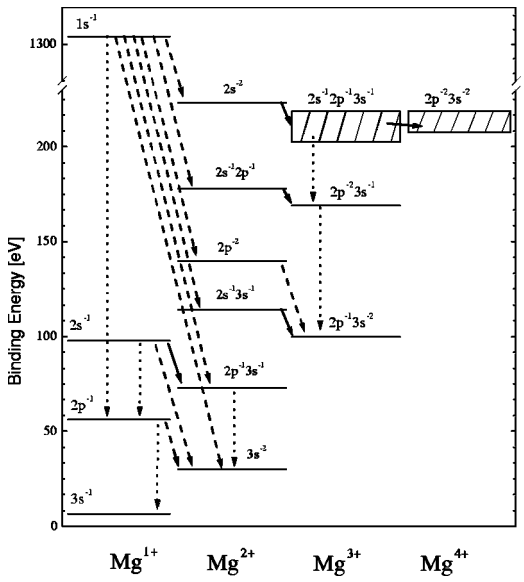

FIG. 1. Simplified energy level scheme for the Mg $1s$, $2s$, and $2p$ decay. Radiative transitions are indicated with dotted lines, Auger transitions with dashed lines, and Coster-Kronig transitions with solid lines.

[3], we calculated the correlations of the core in a more accurate approximation: in the configuration interaction (CI) scheme, solutions of secular equations and natural orbitals for the excited channels [10] were employed. To check the accuracy of the PT calculations, we repeated the calculations on DAP upon the $1s^{-1}$ decay in Ne with PT. The DAP probability due to the correlations of the core calculated with the PT turned out to be 2.7%, while the result obtained by CI was 3%. This gives an estimate of the accuracy of the PT approach employed in this work.

IV. RESULTS AND DISCUSSION

The photoelectron-photoion coincidence method has been applied to study the decay probabilities of the Mg $1s^{-1}$, $2s^{-1}$, and $2p^{-1}$ hole states. The results of this investigation and the comparison to theoretical calculations are described in this section. The decay trees for these three vacancies in Mg calculated in the one-electron configuration-average approximation are shown in Fig. 1. The radiative transitions are indicated with dotted lines, the Auger transitions with dashed lines, and the Coster-Kronig transitions with solid lines. Furthermore, the final ionic charges for each decay path are listed on the x axis.

A. Mg $2s^{-1}$ and Mg $2p^{-1}$

An overview electron spectrum for the excited L shell taken at a photon energy of 173 eV can be seen in Fig. 2. For the sake of intensity needed in the coincidence mode, the electron spectrum was taken with a moderate resolution only. Thus, the $2p^{-1}$ photoelectron peak is not resolved into the fine-structure components. The respective coincidence spectra were taken not only at the maxima of the $2s^{-1}$ and $2p^{-1}$

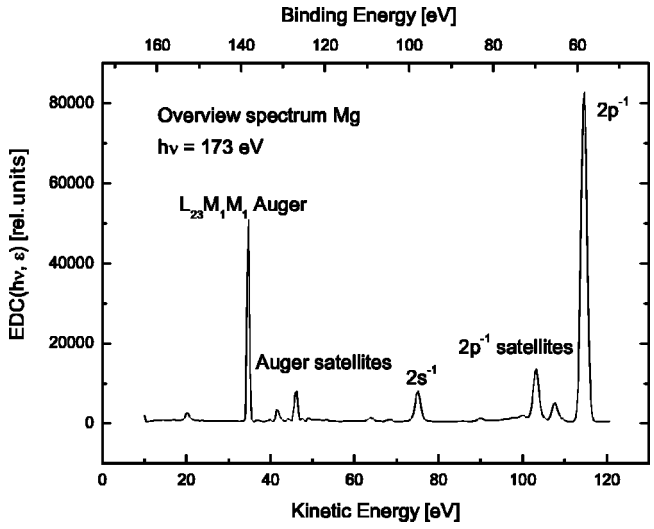

FIG. 2. An overview electron spectrum for the excited Mg $2p$ and $2s$ taken at a photon energy of 173 eV.

photoelectron peaks but also at other electron energies within the peak region and on the background. The advantage of this FIRE spectroscopy has been explained in Sec. II B.

Let us first concentrate on the decay of the Mg $2p^{-1}$ hole state. This hole state is energetically allowed to decay into Mg^{1+} and Mg^{2+}. Figure 3 shows the $2p^{-1}$ photoelectron spectrum with its decomposition into the two FIRE($n+$)

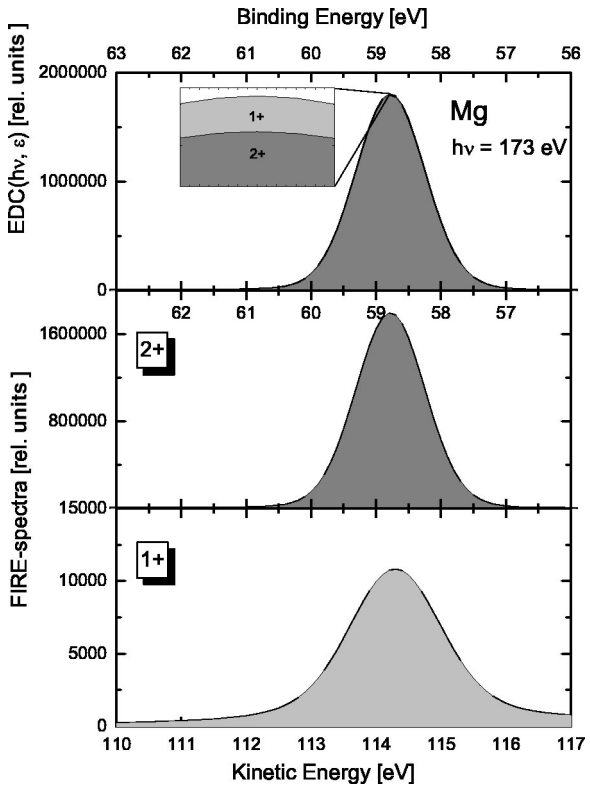

FIG. 3. Top: $2p$ photoelectron spectrum of Mg recorded at a photon energy of 173 eV. Bottom: FIRE($n+$) spectra of the charge states Mg^{1+} and Mg^{2+} (note the change of scale).

TABLE I. Measured and calculated ion yields (in %) upon the decay of $2p$, $2s$, and $1s$ vacancies in Mg. Theory (a) denotes the use of the one-electron configuration-average approximation, whereas Theory (b) stands for the inclusion of electron correlations.

Initial state		Final ion charge 1+	2+	3+	4+
$1s^2 2s^2 2p^5 3s^2$	Experiment	0.9(2)	99.1(2)	0	0
	Theory (a)	0.82	99.18	0	0
$1s^2 2s^1 2p^6 3s^2$	Experiment	$\leqslant 2$	99(2)	$\leqslant 2$	$\leqslant 2$
	Theory (a)	0	100	0	0
	Theory (b)	0	99.24	0.73	0.03
$1s^1 2s^2 2p^6 3s^2$	Experiment	$\leqslant 0.5$	5.1(2)	88.6(3)	6.3(1)
	Theory (a)	0.02	3.98	89.44	6.56

spectra for the two final ionic charge states 1+ and 2+. As can be seen from the lower part of Fig. 3, the $2p^{-1}$ hole state decays predominantly by 99.1(2)% into the Mg^{2+} final state. This final state can only be reached by the $L_{2,3}M_1M_1$ Auger process ($Mg^+ 2p^{-1} \rightarrow Mg^{2+} 3s^{-2} \epsilon l$). The probability for the decay into the Mg^{1+} final state, which takes place via the radiative decay ($Mg^+ 2p^{-1} \rightarrow Mg^{2+} 3s^{-1} + h\nu$), is 0.9(2)%. The deduced decay probabilities agree very well with the ones calculated, i.e., 0.82% for the 1+ and 99.18% for the 2+ final state. The values are listed in the first row of Table I. The probability for the radiative decay can be taken as the average fluorescence yield $\overline{\omega_L}$ of the L shell because the radiative decay probability of the $2s^{-1}$ hole state is negligible, see [12] and our own calculations.

The investigation of the decay of the Mg $2s^{-1}$ hole state showed the sensitivity limit of the coincidence method. Only the detection of the 2+ final state was possible. The upper error limit of the measured values, 0(2)% for the 1+, 3+, and 4+ decay, exceeds the theoretical calculations. The higher sensitivity of the method in the case of the $2p^{-1}$ hole state decay is due to the much higher photopeak intensity which delivers a higher start to pulse rate. Thus, the FIRE spectra could not be evaluated. Figure 4 shows the Mg $2s^{-1}$ coincidence measurements taken at a photon energy of 173 eV. The final ionic charge states of the three stable Mg isotopes [^{24}Mg(78,99%), ^{25}Mg(10.00%), ^{26}Mg(11.01%)] are shown. In the middle, the corresponding reference spectrum of false coincidences and at the bottom, the evaluated spectrum of true coincidences can be seen. The decay probability into the 2+ final ionic state came out to be 99(2)%. The theoretical calculations predict 100% for the 2+ final state in the scheme of the one-electron configuration-average approximation. With the consideration of many-electron correlations, as described in Sec. III, this decay probability is 99.24%.

Furthermore, the production of 3+ and 4+ ions upon the Mg $2s^{-1}$ decay is predicted. For the production of the higher final ionic charge states (3+ and 4+) we considered only the many electron-correlations in the final state of the dominating Coster-Kronig $L_1L_{2,3}M_1$ transition.

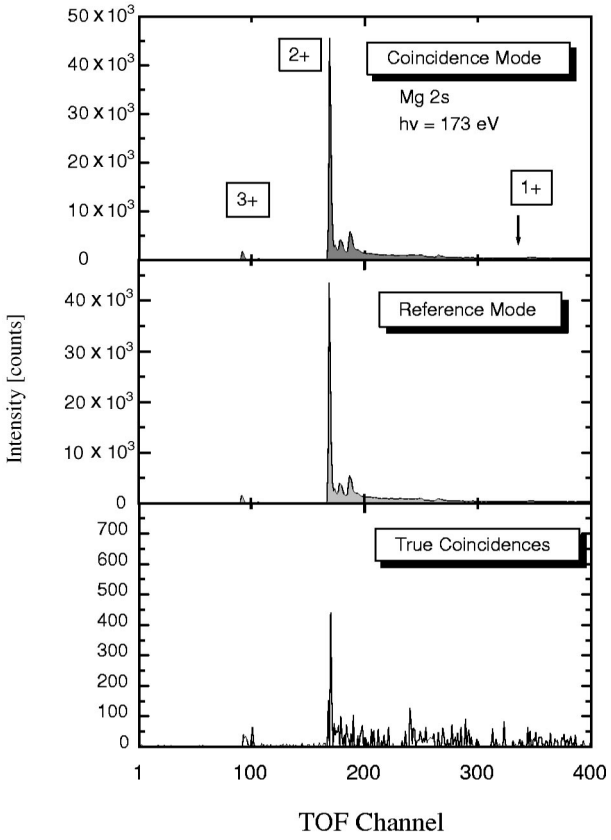

FIG. 4. Mg $2s$ coincidence measurements. Top: measured ion coincidence spectrum recorded at 173 eV photon energy, containing true and false coincidences. Middle: corresponding reference spectrum of false coincidences. Bottom: spectrum of true coincidences.

It should be noted that the two-electron correlations of core electrons which are present both in initial and in final states of a Coster-Kronig transition (for example, $2p2p$-$\{n_1, \epsilon_1\} l_1 \{n_2, \epsilon_2\} l_2$) cancel themselves out in the transition amplitudes between many-configuration states, and do not lead to any multiple processes. This follows from the fact that both the configuration mixing and the Auger transition amplitudes are calculated with the same operator of electrostatic interaction. Inclusion of such correlations only in the initial or only in the final state may lead to severe mistakes. Thus, only those correlations which are absent in the initial state should be considered. Calculated contributions to the production of 3+ and 4+ ions upon the Mg $2s$ vacancy decay are listed in Table II.

B. Mg $1s^{-1}$

In order to investigate the Mg $1s^{-1}$ decay, the photon energy was tuned to 1383 eV. This energy is well above the K-shell ionization energy of 1303 eV to avoid disturbances due to postcollision interaction. Figure 5 shows a coincidence spectrum measured together with its corresponding reference spectrum and the true coincidences evaluated. The final ionic states of 2+, 3+, and 4+ of the three isotopes could be clearly determined. However, the 1+ charges could not be measured which is due to the very low decay prob-

TABLE II. Contributions from various correlations in the state $1s^2 2s^2 2p^5 3s^1 \epsilon_{CK} p$ to the production of 3+ and 4+ ions upon the Coster-Kronig decay of the $2s$ vacancy in Mg.

Correlation type	Excitation	Final ion charge	Probability /%
Monopole shake off	$3s-\epsilon s$	3+	0.1
Core electrons	$2s2s-2p\{n,\epsilon\}p$	4+	0.0072
	$2s2s-3s\{n,\epsilon\}s$	4+	0.0025
	$2s2p-3s\{n,\epsilon\}p$	4+	0.0144
	$2p2p-3s\{n,\epsilon\}p$	3+	0.0046
Core and	$2s\epsilon_{CK}p-\{n,\epsilon_1\}l_1\epsilon_2 l_2$	3+	0.0092
CK electrons	$2p\epsilon_{CK}p-\{n,\epsilon_1\}l_1\epsilon_2 l_2$	3+	0.1672
	$3s\epsilon_{CK}p-\epsilon_1 l_1\epsilon_2 l_2$	3+	0.4619

ability to the 1+ final ionic state. With diagram transitions, the 1+ final ionic state can be reached by cascade processes through $K\alpha$ and subsequent $L\eta$ and Ll transitions ($Mg^+1s^{-1}\rightarrow Mg^+2p^{-1}+h\nu\rightarrow Mg^+3s^{-1}+h\nu$) only.

There are various pathways for the $1s^{-1}$ hole state to decay to higher final ionic states which are indicated in the decay scheme in Fig. 1. Almost all of them are reached by cascade transitions. The 3+ final ionic state is the most probable one. This was to be expected considering the decay probabilities for the $2s^{-1}$ and $2p^{-1}$ decays. The evaluation

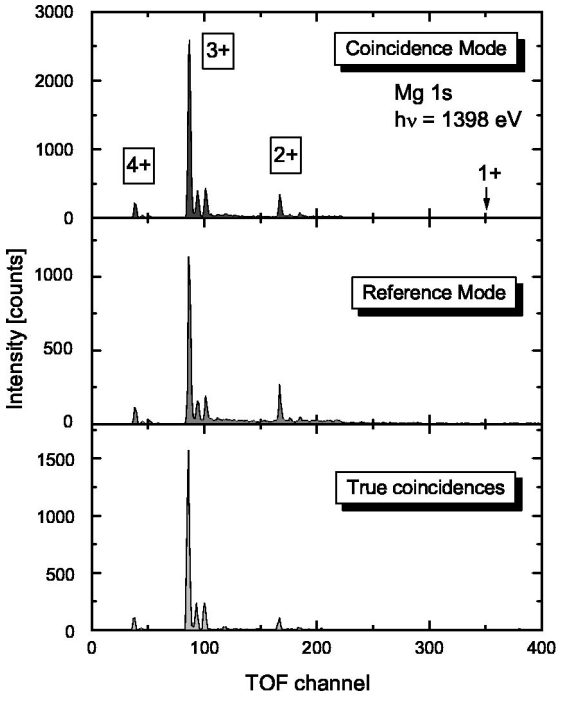

FIG. 5. Mg $1s$ coincidence measurements. Top: measured ion coincidence spectrum recorded at 1398 eV photon energy, containing true and false coincidences. Middle: corresponding reference spectrum of false coincidences. Bottom: spectrum of true coincidences.

of the FIRE spectra gives a decay probability to the 3+ final ionic state of 88.6(3)%. Our calculation gives for 3+ a slightly higher value of 89.44%. Also the calculated 4+ probability of 6.56% agrees very well with the experimental value of 6.3%. In the one-electron configuration-average approximation, the 4+ final ionic state is reached via unique pathway ending up with the $2s^{-1}2p^{-1}3s^{-1}\rightarrow 2p^{-2}3s^{-2}$ Coster-Kronig transition. The peculiarity of the latter is that due to the overlap of the multiplets of the initial and final states, some of the $2s^{-1}2p^{-1}3s^{-1}LS$ states cannot decay into $2p^{-2}3s^{-2}L'S'$ states being lower in their energy. We considered only those $2s^{-1}2p^{-1}3s^{-1}LS$ terms which can be reached from the $2s^{-2}$ state by previous Coster-Kronig transitions. The probabilities of their appearance were taken to be proportional to their statistical weights. In this approximation, the portion of the states of the $2s^{-1}2p^{-1}3s^{-1}$ configuration which do not decay into and end up in the 3+ final ionic state is 0.25. The calculated value for the 2+ decay probability of 3.98% is underestimated in comparison to the experimental value of 5.1%. The two main decay pathways to the 2+ final ionic state are the radiative decay ($K\alpha$ radiation) into a $2p^{-1}$ hole state followed by the Auger decay ($L_{2,3}M_1M_1$) and the Auger decay ($KL_{2,3}M_1$) into the $2p^{-1}2s^{-1}$ double hole state followed by the radiative decay ($L\eta, Ll$). Evidently, either both of these branches or one of them was underestimated in our theory. Hence, the 3+ and 4+ decay probabilities turned out to be relatively higher.

V. SUMMARY

The whole cascade decay of magnesium was investigated by using the photoelectron-photoion coincidence spectroscopy of the $1s^{-1}$, $2s^{-1}$, and $2p^{-1}$ hole states separately. Possible decay routes have been discussed on the basis of one-electron configuration-average approximation calculations. For the $2s^{-1}$ decay, the calculations go beyond this approximation including electron correlations. This is supported by the experimental results. The experimentally determined and calculated decay probabilities for the $1s^{-1}$, the $2s^{-1}$, and the $2p^{-1}$ decay, i.e., the whole cascade, are in good agreement with each other. The underestimation of the decay probability to the 2+ final ionic state by the calculations is mainly due to the underestimation of the K-$L_{2,3}M_1$ and the K-$L_{2,3}$ decay branches.

The investigation of the $2s^{-1}$ and $1s^{-1}$ decays also showed the sensitivity limit of our current coincidence setup. From measurements, the sensitivity for decay probabilities can be estimated to lie in the promille region. This restriction could be overcome by using an electron spectrometer with a higher transmission.

Our investigation also yields some fundamental parameters important for analytical methods such as *x*-ray fluorescence analysis; Namely, the fluorescence yield for the K shell ω_K is 2.47%. In the latest review for fluorescence yields [11], a measured value is given with 2.7(3)% and a best fit value with 2.6%. Thus, our value agrees within the uncertainties assumed very well with these values. Our measured fluorescence yield for the L shell $\bar{\omega}_L$ is 0.9(2)%, which is the yield for the $L\eta$ and Ll transitions. To the best of our knowledge,

this is the first measured value. Hubbell *et al.* [11] indicate an extrapolated fitted value of 0.03%, which is one order of magnitude lower than our result. The same holds for the Coster-Kronig factor of the whole *L* shell, which is the sum $f_{1,2}+f_{1,3}$, which came out to be 98.75%. Here, even calculated or extrapolated fit values cannot be found in the literature.

ACKNOWLEDGMENTS

The authors express their thanks to the staff at BESSY, especially to Ch. Jung, for their assistance. One of the authors (A.G.K.) would like to thank his colleagues from the Laboratoire Cassini UMR 6529 for their hospitality during his stay in Nice where a part of this work was done.

[1] T. Luhmann, Ch. Gerth, M. Martins, M. Richter, and P. Zimmermann, Phys. Rev. Lett. **76**, 4320 (1996).
[2] S. Brünken, Ch. Gerth, B. Kanngießer, T. Luhmann, M. Richter, and P. Zimmermann, Phys. Rev. A **65**, 042708 (2002).
[3] B. Kanngießer, M. Jainz, S. Brünken, W. Benten, Ch. Gerth, K. Godehusen, K. Tiedtke, P. van Kampen, A. Tutay, P. Zimmermann, V.F. Demekhin, and A.G. Kochur, Phys. Rev. A **62**, 014702 (2000).
[4] B. Kanngießer, S. Brünken, K. Godehusen, Ch. Gerth, W. Malzer, M. Richter, and P. Zimmermann, Nucl. Instrum. Methods Phys. Res. A **467-468**, 1477 (2001).
[5] T. Luhmann, Ch. Gerth, M. Groen, M. Martins, B. Obst, M. Richter, and P. Zimmermann, Phys. Rev. A **57**, 282 (1998).
[6] T. Luhmann, Rev. Sci. Instrum. **68**, 2347 (1997).
[7] A.G. Kochur, A.I. Dudenko, V.L. Sukhorukov, and I.D. Petrov, J. Phys. B **27**, 1709 (1994).
[8] A.G. Kochur, V.L. Sukhorukov, A.I. Dudenko, and Ph.V. Demekhin, J. Phys. B **28**, 387 (1995).
[9] A.G. Kochur, A.I. Dudenko, and D. Petrini, J. Phys. B **35**, 395 (2002).
[10] V.F. Demekhin, Ph.V. Demekhin, A.G. Kochur, and N.V. Demekhina, Zh. Strukt. Khim. **39**, 1001 (1998).
[11] J.H. Hubbell, P.N. Trehan, N. Singh, B. Chand, D. Mehta, M.L. Garg, R.R. Garg, S. Singh, and S. Puri, J. Phys. Chem. Ref. Data **23**, 2,339 (1994).
[12] M.O. Krause, J. Phys. Chem. Ref. Data **8**, 2,307 (1979).